

COB-2023-1283

A WEB-BASED SIMULATOR FOR LEAK DETECTION PROBLEMS IN WATER DISTRIBUTION PIPES USING VIBRO-ACOUSTIC TECHNIQUES

Fabício César Lobato de Almeida

Michael John Brennan

Maurício Kiotsue Iwanaga

Sillas de Oliveira César

Luis Armando Ferreira Bispo

Faculty of Engineering of Bauru, UNESP-FEB, Av. Eng. Luís Edmundo Carrijo Coube, 14-01, Bauru - SP, Brazil
e-mails: fabricio.lobato@unesp.br; mjbrennan0@btinternet.com; mkiwanaga23@gmail.com; sillas.cezar@grupoccr.com.br; luis.armando@unesp.br

Oscar Scussel

Institute of Sound and Vibration Research, University of Southampton, Highfield, Southampton SO17 1BJ, UK
e-mail: O.Scussel@soton.ac.uk;

Abstract. *Reduction of non-revenue water is one of the main goals of the water industry. It is estimated that 40% of water pumped via distribution systems in Brazil is lost, but there are states which have losses of 70%. One way of minimizing this problem is by massive investment in replacing old metallic pipes by plastic pipes made from PVC (Polyvinyl Chloride) and HDPE (High Density Polyethylene) material. Furthermore, early detection and location of leaks plays a major role in reducing losses. This can be conducted using vibro-acoustics techniques, but there are problems with plastic pipes compared to metallic pipes, especially when using leak noise correlators. This is because the leak noise that propagates through the pipe is heavily attenuated in plastic pipes reducing the amplitude and distance that this noise can propagate. Leak noise correlators use knowledge of the leak noise velocity and an estimate of the difference between the arrival times of the leak noise at two sensors placed on the pipe at available access points. Generally, the pipe geometry (wall thickness and pipe nominal radius) and its Young's modulus have a profound effect on leak noise attenuation and velocity. Moreover, the surrounding medium also has an additional effect. In this paper some web-based software is described that simulates different scenarios to help users of leak noise correlators to understand the physics behind the problem and to help them select the properties of some filters that need to be set to obtain reliable results. The software is based on a wave-type model which takes into account the pipe vibration response due to excitation by a leak. Inputs to the model are the pipe geometry, material properties of the pipe and surrounding medium, distance between the sensors and sensor type (accelerometer, geophone and hydrophone). These parameters are then used to estimate the leak velocity, time delay, frequency bandwidth (CPSD-Cross-Power Spectral Density) and leak location, which are given in a user-friendly graphical interface.*

Keywords: *leak detection, buried water pipe, correlator, software, wave model*

1. INTRODUCTION

Climate change and high demand of potable water in big cities have increased the need to manage water loss in water distribution systems (Eliasson, 2015; Hamilton and McKenzie, 2014). Recently, long draught seasons have stressed cities around Brazil such as São Paulo city in 2014/2015 (Millington, 2018), which was very close to collapse due to the lack of potable water, and more recently in 2021 (Getirana et al., 2021). This problem, however, is a worldwide issue that affects many countries around the globe (Greve, et al., 2018; Liemberg and Wyatt, 2019). Hence, strategies to reduce non-revenue water have been put in place by water distribution companies (Zaman et al., 2020). These strategies use different technologies to locate leaks in buried water pipes (El-Zahab and Zayed, 2019; Islam et al., 2022). The simplest one is the balance between the pressure vs flow to locate regions where leaks are more likely to be present (Al Qahtani et al., 2020). Many techniques can be applied to refine the search for the leak position. Some of these are invasive, such as smart ball (Fletcher and Chandrasekaran, 2008), and others not invasive like the ground penetrating radar (Cataldo et al., 2014; Abouhamad, Zayed and Moselhi, 2016), thermal analysis (Fahmy and Moselhi, 2009) and more recently satellite imaging (Martins et al., 2019). Furthermore, vibro-acoustic techniques are generally the more popular in leak detection surveys. The simplest vibro-acoustic technique involves a listening stick, which is a metallic rod placed on the pipe, so that the pipe vibration is transmitted through the rod to the "user's ears" (Hamilton and McKenzie, 2014). Similar to the listening stick there are geophones that are placed on the surface right above the buried pipe to detect the leak and estimate its position (Hamilton and McKenzie, 2014). These two techniques rely on user experience and provide a single

measurement only, so that leak detection is subjective and easy to be misinterpret. Leak noise correlators employ a vibro-acoustic technique where at least two sensors are used to pinpoint the position of a leak position (Fuchs and Riehle, 1991; Hamilton and McKenzie, 2014). This technique can be invasive when hydrophones are used, but generally accelerometers are applied which are placed either directly to the pipe wall or any access point where the pipe vibration can be measured, i.e. hydrants (Gao et al., 2004; Almeida et al., 2014). Leak noise correlators use knowledge of the leak noise velocity and an estimate of the difference between the arrival times of the leak noise at two sensors placed on the pipe at available access points. It needs a good estimation of the time delay and leak velocity to successfully pinpoint the leak position (ADS, 2010; Aquasave, 2015; FUJI TECOM, 2022). Although it seems straight forward, the user has to set up filters prior to calculate the time delay estimation together with defining the pipe properties to estimate the leak velocity (Gao et al., 2004). In most cases, commercial leak noise correlators do not take into account the effects of the surrounding medium on the leak noise, which has a direct effect on the leak noise attenuation (filter bandwidth) and velocity (Brennan et al., 2018). This paper describes some web-based software developed to aid professionals that use leak noise correlators. The software is based on a wave model that accounts for the pipe properties (material and geometry), surrounding medium (soil type) and sensor (hydrophone, geophone or accelerometer) used to measure pipe vibration or acoustic pressure due to a leak. These inputs are provided by the user, so that a normalized modulus of the cross-power spectral density (CPSD), the phase, normalized cross-correlation and leak velocity estimation are provided as the software outputs. The first is used to estimate the frequency bandwidth over which the leak energy is mostly located. The phase and normalized modulus of the cross-correlation function are used to estimate the time delay in the frequency and time domains, respectively. Finally, the leak noise velocity is estimated via the wave-speed that carries most of the leak energy (Pinnington and Briscoe, 1994; Brennan et al., 2018; Scussel et al., 2023). These simulations are performed using two different user-friendly interfaces. The results provided by the web-based software are compared to actual leak noise data to show this software is representative of actual situations and can be used to aid leak detection teams.

2. CLASSIC SIGNAL PROCESSING FOR TIME DELAY ESTIMATION

As mentioned previously, a leak noise correlator uses the estimation of the time of arrival between the leak excitation signal collected via at least two sensors placed at available access points. Moreover, the speed at which the leak noise propagates along the pipe is also used to pinpoint the leak position. Figure 1 shows a schematic depicting how the leak noise energy is dissipated along the pipe and into the surrounding medium. The model is discussed in the next section. This section focuses on the signal processing used to estimate the time delay and leak velocity.

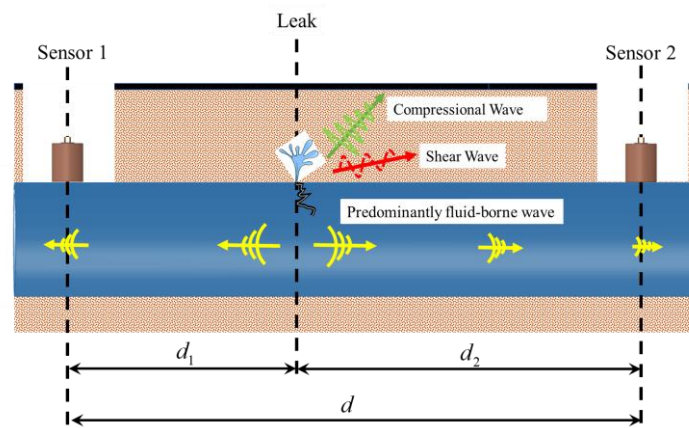


Figure 1. Schematic diagram depicting how the leak energy propagates along the pipe and radiates throughout the soil via different wave types.

The leak position with reference to sensor 1 is given by (Gao et al., 2004):

$$d_1 = \frac{d - cT_o}{2}, \quad (1)$$

where d is the total distance between the sensors in metres, c is the leak velocity in m/s and T_o is the time of arrival or the time delay in seconds between $x_1(t)$ and $x_2(t)$.

The process of time delay estimation has a few steps. First it is important to perform the calculation of the Cross Power Spectral Density (CPSD) function, which can be used to observe the power distribution of the signal over a frequency range. This distribution can be used to provide an initial estimation of the frequency range where the leak signal is likely

to be located in practice. This estimation is used to set up a bandpass filter prior to the calculation of the time delay via the cross-correlation function. The CPSD function $S_{x_1x_2}(\omega)$ is defined as (Shin and Hammond, 2008):

$$S_{x_1x_2}(\omega) = \lim_{T \rightarrow \infty} \frac{E[X_1^*(\omega)X_2(\omega)]}{T}, \quad (2)$$

where $E[\cdot]$ is the expectation operator, $X_1(\omega)$ and $X_2(\omega)$ are the Fourier transforms of $x_1(t)$ and $x_2(t)$ respectively, $*$ denotes complex conjugate, ω frequency in rad/s, and T is the time duration of a signal segment. Note that $S_{x_1x_2}(\omega)$ can be written as $|S_{x_1x_2}(\omega)|e^{j\phi(\omega)}$ in which $|S_{x_1x_2}(\omega)|$ is the modulus of the CPSD, $\phi(\omega)$ is the phase between the two signals at frequency ω and $j = \sqrt{-1}$. If there is a pure delay in the system (buried pipe excited by a leak), then $\phi(\omega) = \omega T_0$. It is important to note that the CPSD contains modulus and phase information, where the first can be used to estimate the frequency bandwidth as mentioned previously, and the latter is used to estimate the time delay (time of arrival) between the signals $x_1(t)$ and $x_2(t)$. These signals are collected using sensors, generally placed at pipe access points (Gao et al., 2004).

The cross-correlation function between the measured signals $x_1(t)$ and $x_2(t)$ whose means are set to zero, is given by (Shin and Hammond, 2008):

$$R_{x_1x_2}(\tau) = E[x_1(t)x_2(t+\tau)], \quad (3)$$

where τ is the delay. The delay that results in the highest similarity between the two signals $x_1(t)$ and $x_2(t)$ (indicated by a peak in the cross-correlation function) is considered to be an estimate of the time delay (T_0) between these signals. The cross-correlation function is also related to the Fourier Transform of the CPSD function by (Shin and Hammond, 2008):

$$R_{x_1x_2}(\tau) = \int_{-\infty}^{+\infty} S_{x_1x_2}(\omega)e^{j\omega\tau} d\omega. \quad (4)$$

The leak velocity can be calculated via standard tables which come with commercial correlators or via analytical equations. The latter is based on wave models being one of which described in the next section. This is the same model used in the web-based software introduced in this work.

3. WAVE MODEL OVERVIEW

The CPSD between the two signals $x_1(t)$ and $x_2(t)$ for a buried water pipe can also be estimated using the system's Frequency Response Function (FRF) and the leak spectrum characteristics $S_{ll}(\omega)$ (Scussel et al., 2021) by

$$S_{x_1x_2}(\omega) = S_{ll}(\omega)H_1^*(\omega, d_1)H_2(\omega, d_2), \quad (5)$$

where $H_1(\omega, d_1)$ and $H_2(\omega, d_2)$ are the FRFs of the pipe sections with length d_1 and d_2 , respectively. Furthermore, to simplify the model the leak spectrum is assumed to have white noise characteristics (Gao et al., 2004), hence $S_{ll}(\omega) = S_o$. The pipe model FRF used in this paper assumes that the leak noise energy is transmitted along the pipe via a predominantly fluid-borne wave, in which there is strong coupling between the fluid and the pipe wall (Pinnington and Briscoe, 1994; Muggleton, Brennan and Pinnington, 2002). This wave is shown in Figure 1 and its main characteristic is that either acoustic (i.e. hydrophones) or vibration (i.e. accelerometers/geophones) sensors can be used with leak noise correlators. Furthermore, the leak energy can also radiate through the soil via shear and compressional waves, also depicted in Figure 1. These two mechanisms can occur simultaneously in the system when the soil presents a sandy-like characteristic, but only compressional waves are present in stiff clay-like soils as discussed by Brennan et al. (2018). Thus, the surrounding medium and the pipe material have a direct effect on the leak energy attenuation and velocity in the pipe. This is taken into account in the model herein described. The FRF for the pipe is given by (Gao et al., 2005)

$$H(\omega, x) = (j\omega)^n e^{-j\omega x/c} e^{-\omega\beta x}, \quad (6)$$

where x is the distance from the leak position to any measurement position, i.e. d_1 or d_2 , $c = \omega/\text{Re}\{k\}$, $\beta = -\text{Im}\{k\}/\omega$ is related to the wave attenuation, and k is the wavenumber of the predominantly fluid-borne wave. The term $(j\omega)^n$ is related to the type of sensor used for collecting the pipe response, so n can be set to 0, 1 or 2 for pressure/displacement, velocity and acceleration measurements, respectively. It is important to note that the attenuation is a function of d . The wavenumber is given by Scussel et al. (2023):

$$k = k_w \left(1 + \frac{K_w}{K_p + K_{p-m} + K_m} \right)^{1/2}, \quad (7)$$

where $k_w = \omega/c_w$, is the free water wavenumber in which $c_w=1500$ m/s is the speed of sound in water, and $K_w = (2B_w/a)/\left[\left(k^2/k_w^2\right)-1\right]$, $K_p = E_p^*b/[a^2(1-\nu_p^2)]-\omega^2\rho_p b$, $K_{p-m} = (\bar{K}_p + \bar{K}_m)^2/(\tilde{K}_p + \tilde{K}_m)$ and K_m are, respectively, the wave dynamic stiffnesses of the water, pipe, interaction between pipe and surrounding medium and the dynamic stiffness of the surrounding medium (soil); B_w is the bulk modulus of water, $B_m^* = B_m(1+j\eta_d)$ and $G_m^* = G_m(1+j\eta_s)$ are the complex shear and bulk moduli of the surrounding medium (soil) respectively, in which G_m is the shear storage modulus, η_s is the shear loss factor, B_m is the Bulk modulus and η_d is the compressional loss factor; the pipe geometry and material properties are given by the mean radius a , the wall thickness b , the density ρ_p , and the complex Young's modulus $E_p^* = E_p(1+j\eta_p)$ in which E_p is the storage modulus and η_p the loss factor. Furthermore, it can be seen that K_{p-m} involves several terms, which are given by (Scussel et al., 2023):

$$\bar{K}_p = iv_p k E_p^* b / [a(1-\nu_p^2)], \quad (8)$$

$$\bar{K}_m = j(2-\alpha\bar{H}_d k), \quad (9)$$

$$\tilde{K}_p = k^2 E_p^* b / (1-\nu_p^2) - \omega^2 \rho_p b, \quad (10)$$

$$\tilde{K}_m = j(2-\alpha\bar{H}_d k), \quad (11)$$

where $\alpha = k_s^2/(k_d^R k_s^R \bar{H}_s + k^2 \bar{H}_d)$, $\bar{H}_s = H_0(k_s^R r)/H'_0(k_s^R r)$, in which $H_0(\cdot)$ is a Hankel function of the second kind of zero order related to conical waves that radiate throughout the soil, ' denotes a spatial derivative, r is the radial distance from the pipe center, and the superscript R denotes the radial direction; $k_s^R = \sqrt{k_s^2 - k^2}$, where $k_s = \omega/c_s$ is the shear wavenumber for the soil and $c_s = \sqrt{G_m^*/\rho_m}$ is the related wave speed; $k_d^R = \sqrt{k_d^2 - k^2}$, in which $k_d = \omega/c_d$ is the compressional/dilatational wavenumber for the soil and $c_d = \sqrt{(B_m^* + 4G_m^*/3)/\rho_m}$ is the related wave speed. The medium stiffness is given by

$$K_m = \frac{2}{a} + \alpha \frac{k_s^R}{k_d^R} \bar{H}_s \bar{H}_d k_d^R. \quad (12)$$

Hence, the cross-correlation function for the model is computed as,

$$R_{x_1 x_2}(\tau) = S_o \int_{-\infty}^{+\infty} W(\omega) H_1^*(\omega, d_1) H_2(\omega, d_2) e^{(j\omega\tau)} d\omega, \quad (13)$$

where $W(\omega)$ is the FRF of the filter used prior to perform the correlation. The limits of such filter are given by analyzing the modulus of the CPSD. This will be covered in the next section when the web-based software interface is introduced.

4. THE WEB-SOFTWARE INTERFACE

The web-software can be accessed at the link www.correlator.feb.unesp.br, and it has two interfaces. One named as *frequency bandwidth estimation for leak noise correlators*, which is shown in Figure 2(a). The other one is named as *cross-correlation and phase estimation for correlators* is depicted in Figure 2(b). The inputs for both interfaces are:

- Pipe material properties [E_p^* and ρ_p]: This can be PVC (Polyvinyl Chloride), MDPE (High Density Polyethylene), Cast Iron and Concrete. The default values for each material used in the simulator is given in Table 1.
- Sensor Type [$(j\omega)^n$]: hydrophone ($n = 0$, pressure/displacement measurements), geophone ($n = 1$, velocity measurements) and accelerometers ($n = 2$, acceleration measurements).
- Soil Type [B_m^* and G_m^*]: sandy, clay and air (no surrounding medium). The default values for each soil type used in the simulator is given in Table 2.
- Pipe geometry properties [a and b].
- Distance between the sensors [d].

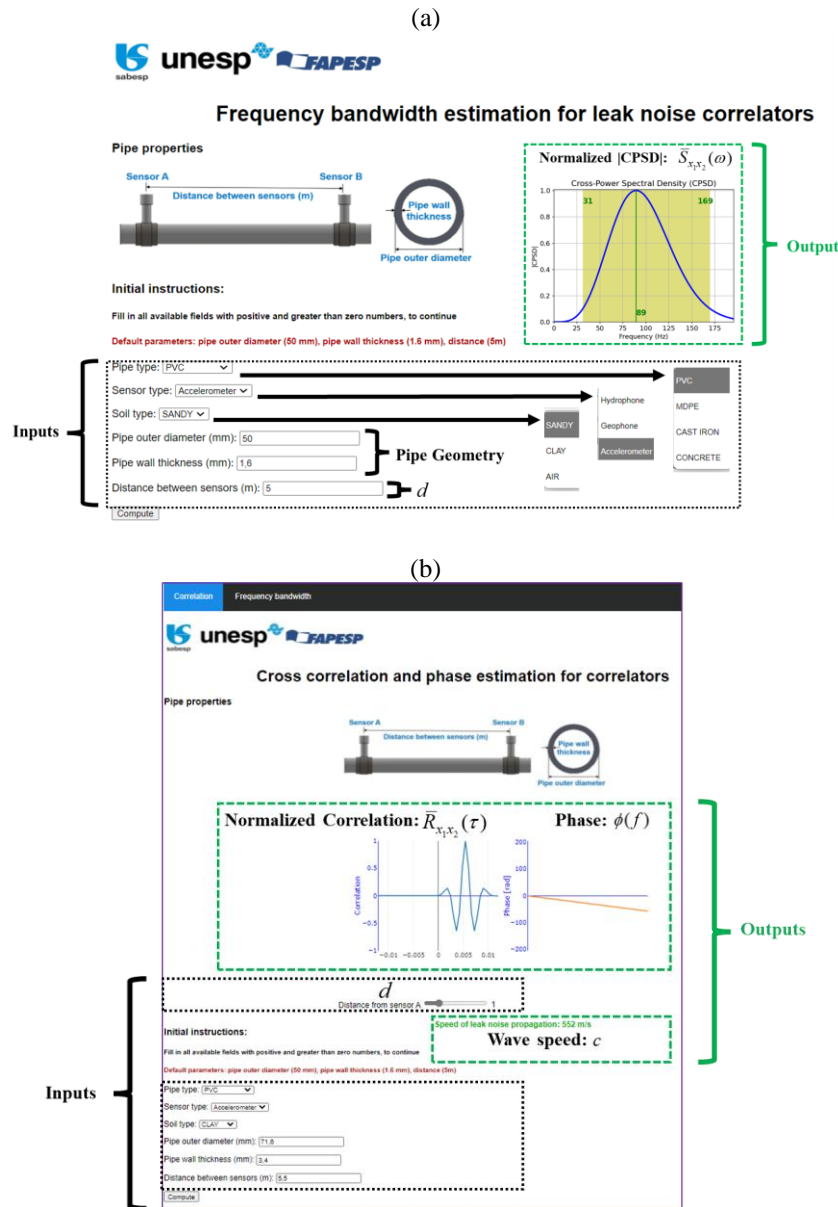


Figure 2. User-friendly interfaces of the web-based software (a) Interface is named as frequency bandwidth estimation for leak noise correlators. (b) Interface named as cross-correlation and phase estimation for correlators.

Table 1. Pipe properties used in the web-based software.

Soil Type Properties	Young's Modulus (N/m ²)	Density (kg/m ³)	Loss Factor	Poisson
PVC	4 10 ⁹	1450	0.06	0.4
MDPE	2 10 ⁹	930	0.06	0.4
Cast Iron	170 10 ⁹	7800	0.001	0.25
Concrete	20 10 ⁹	2240	0.06	0.205

Table 2. Soil properties used in the web-based software.

Soil Type Properties	Bulk Modulus (N/m ²)	Density (kg/m ³)	Shear Modulus (N/m ²)
Sandy	4.7 10 ⁷	2 10 ³	1.5 10 ⁷
Clay	4.5 10 ⁹	2 10 ³	2.4 10 ⁸

The water in the pipe has a the bulk modulus given by B_w which is $2 \cdot 10^9$ N/m². The output for the frequency bandwidth interface is the modulus of the CPSD normalized by its largest value, so that $|\bar{S}_{x_1x_2}(\omega)| = |S_{x_1x_2}(\omega)| / \max[S_{x_1x_2}(\omega)]$. The lower and upper limits of the filter are defined when the $|\bar{S}_{x_1x_2}(\omega)| \geq 0.1$. This is depicted in Figure 2(a) as the software output. The frequency limits are also highlighted and the frequency range over which the CPSD is useful is shaded in the graph. The frequency where the $|\bar{S}_{x_1x_2}(\omega)|$ is maximum is also highlighted for convenience. It is important to note that this is the frequency range estimation where the leak noise is likely to be located, so that the frequency range over which the time delay information can be found.

The same inputs are used for the second interface where the outputs are the normalized cross-correlation, phase and wave speed. The cross-correlation is also normalized by its maximum value (peak), so that $\bar{R}_{x_1x_2}(\tau) = R_{x_1x_2}(\tau) / \max[R_{x_1x_2}(\tau)]$. The distance between the sensors, however, is updated via a sliding bar, so that the phase and the normalized cross-correlation can be performed instantly according to this input. Such tool can be useful to show how the correlation and phase works according to the leak position (closer or further from one sensor, i.e. sensor 1). It is important to note here that the wave-speed calculated in this interface is the predominantly fluid-borne wave affected by the surround medium and pipe properties. This is related to the leak velocity calculated via analytical equations or given by the standard tables.

5. SIMULATIONS

The simulations presented in this section are compared to actual leak data collected in two different test rigs to show the good agreement between the simulated data provided by the web-based software and the data collected from those test rigs. Figures 3(a) and 3(b) respectively show the test rig located in Brazil and the test rig located in the UK. More information about the test rig in Brazil can be found in Brennan et al. (2018), and more information of the test rig in the UK can be found in Almeida et al. (2014). The two main differences between these test rigs are the surrounding medium, and the pipe material and geometry. Table 3 summarizes such characteristics, so that it is possible to conduct two different analyses via the web-based software for these two scenarios. Accelerometers were used to collect the pipe vibration in both test rigs.

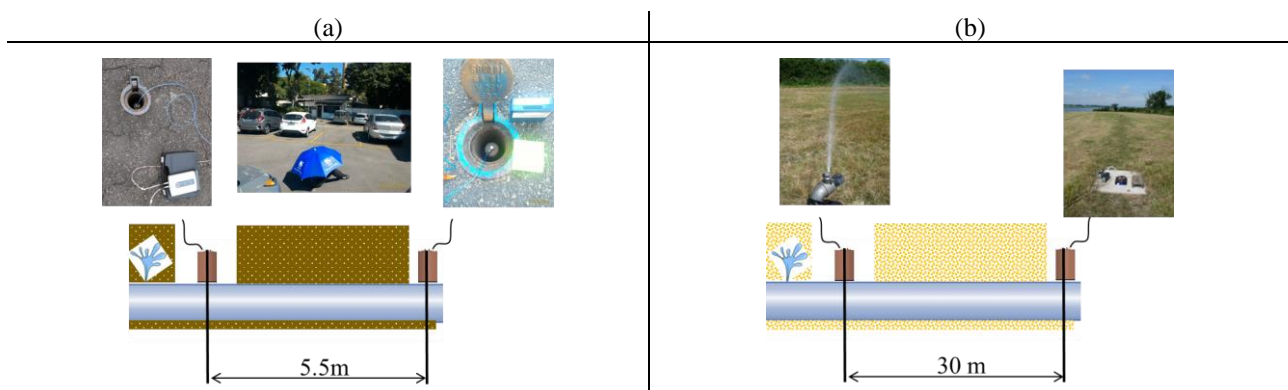


Figure 3. Data collected in the test rig (a) located in Brazil and the test rig (b) located in the UK to show how representative is the data generated by the web-based software.

Table 3. Test rig characteristics.

Test Rig	Soil Type	Pipe Material	Pipe Radius (mm)	Pipe Wall Thickness (mm)	Distance between the sensors (m)
Brazil	Clay	PVC	35.8	3.4	5.5
UK	Sandy	HDPE	84.5	11	30

Figures 4(a), 4(b) and 4(c) show the normalized modulus of the CPSD, the phase and the normalized cross-correlation for the test rig in Brazil and the UK, respectively. The blue thick lines are related to the simulated data provided by the web-based software and the red thin lines are related to the actual leak data. The simulated phase given by the straight line $\phi(\omega) = \omega T_0$ is depicted in dashed blue line for the simulated data to highlight the very good agreement to the actual data. The threshold value of 0.1 for the normalized modulus of the CPSD used to estimate the frequency bandwidth (shaded area) is also depicted in the figure for convenience.

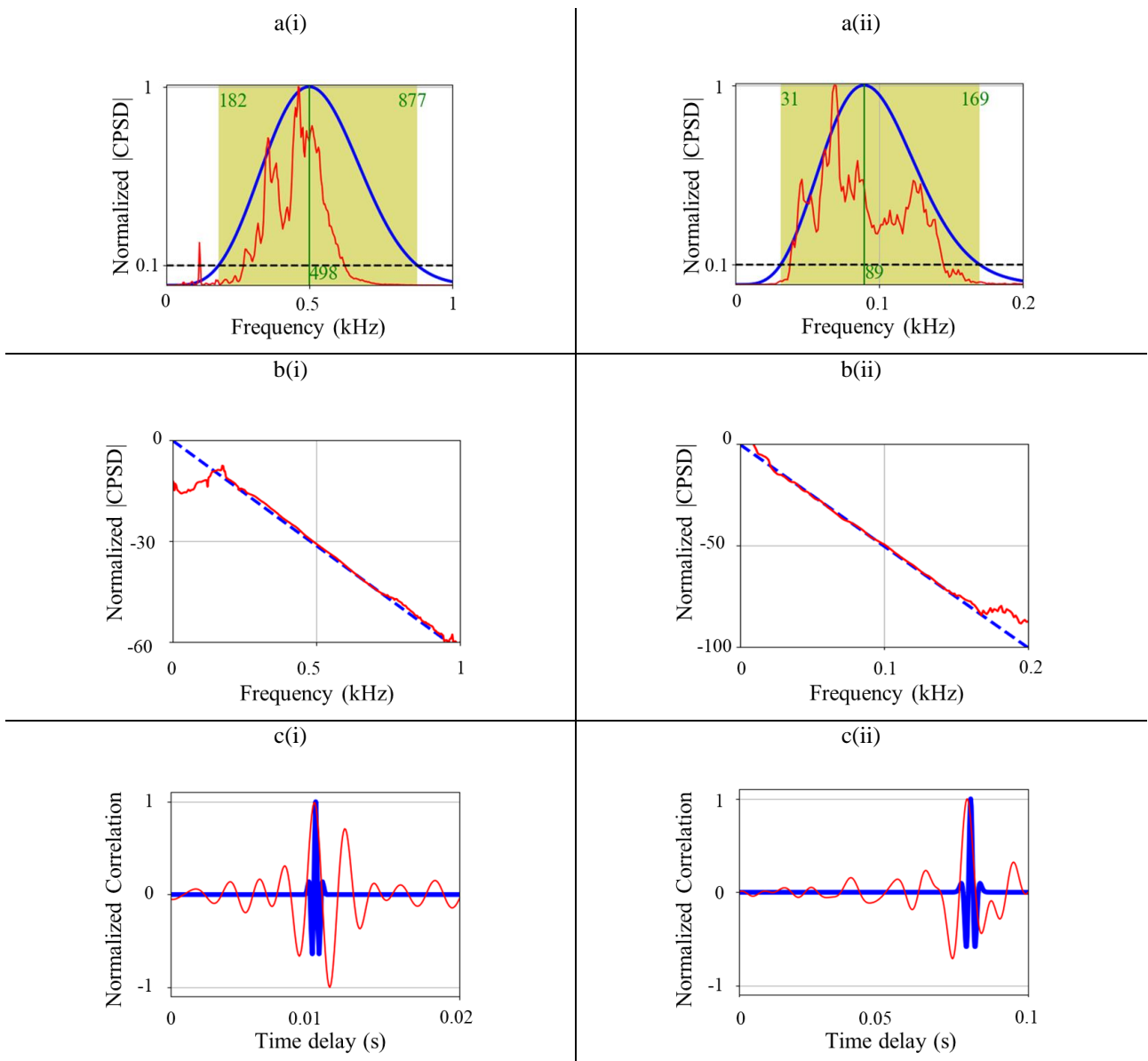


Figure 4. Comparison between the actual data collected from “i” the test rig in Brazil and “ii” the test rig in the UK and the results provided by the web-based software for the (a) Normalized modulus of the CPSD, (b) the unwrapped phase and (c) the normalized cross-correlation. The thick blue lines are related to the simulated data provided by the web-based software and the thin red lines are related to the actual leak data. The simulated phase is depicted as dashed blue lines for convenience.

Although the actual normalized modulus of the CPSD is a bit erratic, it is observed that the actual data is contained within the frequency range given by the simulations. This can be useful for leak noise correlator users to check if the selection of the filter bandwidth is in accordance to the one in actual situations. Moreover, this can be used to check if the bandwidth is too narrow for a specific situation (for a given input), such that leak noise correlators may not be effective in pinpointing the leak. Although the actual normalized cross-correlation is not smooth as with the simulation, there is good agreement concerning the peak (time delay), which corresponds to the phase gradient (the analytical one overlays very well to the actual phase).

6. CONCLUSIONS

This paper has described some web-based software which can aid leak detection professionals which are using commercial leak noise correlators. The model behind the software is based on the wave approach taking into account the buried pipe properties (pipe material and pipe geometry) and the surrounding medium (soil type). Furthermore, this model is related to the predominantly fluid-borne wave which is responsible for propagating leak noise energy in the pipe. Hence, measurements in the water (acoustic pressure) or on the pipe wall (displacement, velocity and acceleration) can be simulated. The speed of such a wave is the one calculated in commercial leak noise correlators. The surrounding medium affects this velocity and the frequency range over which the leak noise information is located. This frequency range is important in the calculation time delay and the wave-speed and is estimated from the normalized modulus of the cross-power spectral density (CPSD) and the associated phase. It is important to note that the inputs for the web-based software are the pipe properties, the surrounding medium properties, the distance between the sensors and the sensor type, and one key output is the CPSD. The results provided by the web-based software have been compared to actual leak data collected from two different test rigs using accelerometers. It has been shown that despite the actual data presents an erratic behavior, the bandwidth, time delay and wave speed (leak velocity) have good agreement to the ones provided by the software.

7. ACKNOWLEDGEMENTS

The authors gratefully acknowledge the financial support provided by the São Paulo Research Foundation (FAPESP) under Grant numbers 2018/25360-3 and 2020/12251-1, and the Coordination for the Improvement of Higher Education Personnel (CAPES) under Grant numbers 432272/2018-6 and 88887.374001/2019-00. The authors also would like to thank the Brazilian water and waste management company (SABESP) for the financial support and test rig facilities provided without which this project would not be possible. The authors gratefully acknowledge the financial support provided by Engineering and Physical Sciences Research Council (EPSRC) under RAINDROP project (EP/V028111/1),

8. REFERENCES

- Abouhamad, M., Zayed, T. and Moselhi, O., 2016. "Leak detection in buried pipes using ground penetrating radar – A comparative study". In: *Pipelines 2016: Out of Sight, Out of Mind, Not Out of Risk*, ASCE, p. 417-424.
- ADS, 2010. *Eureka2R leak noise correlator user manual*, <https://www.adsenv.com/sites/default/files/manuals/adseureka2rusermanuala1.pdf>. Accessed 10 July, 2023.
- Al Qahtani, T., Yaakob, M.S., Yidris, N., Sulaiman, S., Ahmad, K.A., 2020. "A review on water leakage detection method in the water distribution network". *Journal of Advanced Research in Fluid Mechanics and Thermal Sciences*, Vol. 68, n. 2, p. 152-163.
- Almeida, F., Brennan, M., Joseph, P., Whitfield, S., Dray, S., and Paschoalini, A., 2014. "On the Acoustic Filtering of the Pipe and Sensor in a Buried Plastic Water Pipe and its Effect on Leak Detection: An Experimental Investigation". *Sensors*, Vol. 14, p. 5595-5610.
- Aquasave, 2015. *Leak detection*, <http://www.aquasave.mk/en-GB/Home/ServiceDetails/15>. Accessed 10 July, 2023.
- Brennan, M.J., Karimi, M., Muggleton, J.M., Almeida, F.C.L., Lima, F.K., Ayala, P.C., Obata, D., Paschoalini, A.T., Kessissoglou, N., 2018. "On the effects of soil properties on leak noise propagation in plastic water distribution pipes." *Journal of Sound and Vibration*, Vol. 427, p. 120-133.
- Cataldo, A., Persico, R., Leucci, G., De Benedetto, E., Cannazza, G., Matera, L. and De Giorgi, L., 2014. "Time domain reflectometry, ground penetrating radar and electrical resistivity tomography: A comparative analysis of alternative approaches for leak detection in underground pipes". *NDT & E International*, Vol. 62, p. 14-28.
- Eliasson, J., 2015. "The rising pressure of global water shortages". *Nature*, Vol. 517, p. 6.
- El-Zahab, S. and Zayed, T., 2019. "Leak detection in water distribution networks: an introductory overview". *Smart Water*, Vol. 4, n. 5.
- Fahmy, M., and Moselhi, O., 2009. "Detecting and locating leaks in underground water mains using thermography". In *International Symposium on Automation and Robotics in Construction – ISARC 2009*, Austin, United States of America.

- Fletcher, R. and Chandrasekaran, M., 2008. "SmartBall™: A New Approach in Pipeline Leak Detection". In *Proceedings of the 7th International Pipeline Conference 2008*, ASME, Calgary, Alberta, Canada.
- Fuchs, H.V. and Riehle, R., 1991. "Ten years of experience with leak detection by acoustic signal analysis". *Applied Acoustics*, Vol. 33, n. 1, p. 1-19.
- FUJI TECOM, 2022. *Water Leak Detection LC-5000*, <https://www.fujitecom.com/products/pcl.html>. Accessed 10 July, 2023.
- Gao, Y., Brennan, M.J., Joseph, P.F., Muggleton, J.M. and Hunaidi, O., 2004. "A model of the correlation function of leak noise in buried plastic pipes". *Journal of Sound and Vibration*, Vol. 277, n. 1-2, p. 133-148.
- Gao, Y., Brennan, M.J., Joseph, P.F., Muggleton, J.M. and Hunaidi, O., 2005. "On the selection of acoustic/vibration sensors for leak detection in plastic water pipes". *Journal of Sound and Vibration*, Vol. 283, n. 3-5, p. 927-941.
- Getirana, A., Libonati, R. and Cataldi, M., 2021. "Brazil is in water crisis — it needs a drought plan". *Nature*, Vol. 600, p. 218–220.
- Greve, P., Kahil, T., Mochizuki, J., Schinko, T., Satoh, Y., Burek, P., Fischer, G., Tramberend, S., Burtscher, R., Langan, S. and Wada, Y., 2018. "Global assessment of water challenges under uncertainty in water scarcity projections". *Nature Sustainability*, Vol.1, p.486–494
- Hamilton, S. and McKenzie, R., 2014. *Water management and water loss*. IWA Publishing, 2014.
- Islam, M.R., Azam, S., Shanmugan, B., Mathur, D., 2022. "A review on current technologies and future direction of water leakage detection in water distribution network". *IEEE Access*, Vol. 10, p. 107177-107201.
- Liemberg, R. and Wyatt, A., 2019. "Quantifying the global non-revenue water problem". *Water Supply*, Vol. 19, n. 3, p. 831-837.
- Martins, R., Azevedo, A., Fortunato, A.B., Alves, E., Oliveira, A. and Carvalho, A., 2019. "An Innovative and Reliable Water Leak Detection Service Supported by Data-Intensive Remote Sensing Processing". In *International Conference on Computational Science – ICCS 2019*, Lecture Notes in Computer Science, Vol. 11539. Springer.
- Muggleton, J.M., Brennan, M.J. and Pinnington, R.J., 2002. "Wavenumber prediction of waves in buried pipes for water leak detection". *Journal of Sound and Vibration*, Vol. 249, n. 5, p. 939-954.
- Millington, N., 2018. "Producing water scarcity in São Paulo, Brazil: The 2014-2015 water crisis and the binding politics of infrastructure". *Political Geography*, Vol. 65, p. 26-34.
- Pinnington, R.J. and Briscoe, A.R., 1994. "Externally applied sensor for axisymmetric waves in a fluid filled pipe". *Journal of Sound and Vibration*, Vol. 173, n. 4, p. 503-516.
- Scussel, O., Brennan, M.J., Almeida, F.C.L., Muggleton, J.M., Rustighi, E. and Joseph, P.F., 2021. "Estimating the spectrum of leak noise in buried plastic water distribution pipes using acoustic or vibration measurements remote from the leak". *Mechanical Systems and Signal Processing*, Vol. 147, p. 107059.
- Scussel, O., Brennan, M.J., Almeida, F.C.L., Iwanaga, M.K., Muggleton, J.M., Joseph, P.F., Gao Y., 2023. "Key Factors That Influence the Frequency Range of Measured Leak Noise in Buried Plastic Water Pipes: Theory and Experiment". *Acoustics*, vol. 5, p. 490-508.
- Shin K. and Hammond, J.K., 2008. *Fundamentals of signal processing for sound and vibration engineers*, Chichester, Wiley.
- Zaman, D., Tiwari, M.J., Gupta, A.K.; Sen, D., 2020. "A review of leakage detection strategies for pressurized pipeline in steady-state". *Engineering Failure Analysis*, Vol. 109, p. 104264.

9. RESPONSIBILITY NOTICE

The authors are the only responsible for the printed material included in this paper.